Journal of Molecular Structure 922 (2009) 51–57

Contents lists available at ScienceDirect

Journal of Molecular Structure

journal homepage: www.elsevier.com/locate/molstruc

Synthesis, spectral, thermal and theoretical studies of Cu(II) complexes with 3-[4′-dimethylaminophenyl]-1-(2-pyridyl)prop-2-en-1-one (DMAPP)

M. Gaber, S.A. El-Daly, Y.S.Y. El-Sayed *

Chemistry Department, Faculty of Science, Tanta University, El-Bahre Street, Tanta 11113, Egypt

ARTICLE INFO

Article history:
Received 26 March 2008
Received in revised form 10 January 2009
Accepted 20 January 2009
Available online 31 January 2009

Keywords:
Chalcones
Complexes
Spectral
Thermal studies
Effect of viscosity on the complexes

ABSTRACT

Cu(II) complexes of 3-[4′-dimethylaminophenyl]-1-(2-pyridyl) prop-2-en-1-one (DMAPP) are prepared and characterized by elemental analysis as well as spectral studies (IR and UV–vis), ESR, magnetic susceptibilities and thermal studies. The effect of different alcoholic solvents as well as the temperature on the complex formation is studied. The effect of Cu(II) ion on the emission spectrum of the free chalcone is also assigned. The stoichiometry, stability constant, absorption maximum and molar absorptivity of the metal complexes as well as the effect of pH, temperature on complex formation are determined spectrophotometrically. Adherence to Beer's law and Ringbom optimum concentration ranges are determined. The thermal decomposition of the metal complexes is studied by TGA technique. The kinetic parameters like activation energy, pre-exponential factor and entropy of activation are estimated. The structure of complexes was energetically optimized through molecular mechanics applying MM$^+$ force field coupled with molecular dynamics simulation.

1. Introduction

Chalcones, the bichromophoric molecules separated by a keto-vinyl chain, constitute an important class of naturally occurring flavonids exhibiting a wide spectrum of biological activities [1–3]. Also, chalcones have potential applications as artificial sweeteners, new drugs and agrochemicals [4–6]. The importance of this class of compounds is not only due to their biological activities but also to their colors, usually give yellow to orange colors to the tissues in which they are located [2,7]. So, they are attractive to insects in such a way that they contribute to the flower's pollination [8]. In addition, chalcones are widely used for various optical applications including second harmonic generation materials in non-linear optics [9], photorefractive polymers [10], holographic recording materials [11] and fluorescent probes for sensing of metal ions [12–15]. Therefore, the photophysical properties of chalcones containing alkyl amino groups as electron donors have been studied by numerous researchers [16–21]. In an earlier work, the photophysical properties, excitation energy transfer and laser activity of DMAPP. The photophysical properties such as singlet absorption, molar absorptivity, fluorescence spectra, fluorescence quantum yield (ϕ_f) and transition dipole moment (μ_{12}) of DMAPP were measured in different media [22].

In this paper, we are reporting the synthesis and spectroscopic characterization as well as magnetic and conductance measurements of Cu(II) complexes with chalcone ligand (DMAPP) Fig. 1.

2. Experimental

The ligand (DMAPP) was synthesized and characterized according to the method reported previously [22]. All the chemicals used were of Analar grade. Solvents were purified according to standard procedures before use.

2.1. Synthesis of metal complexes

A solution of the appropriate metal ion (0.01 mol) in ethanol (10 ml) was mixed with a solution of the chalcone (0.01 mol) in the same solvent (30 ml) and the resulting mixture was stirred under reflux for 12 h where upon the complexes precipitated after cooling. The solid complexes were then filtered off, washed several times with ethanol, dried and kept in desiccators over dried silica gel. The analytical and spectral data are collected in Table 1.

2.2. Measurements

Microanalyses of C, H and N were made using Heraeus CHN elemental analyzer. The IR spectra were recorded as KBr discs on a Perkin Elmer 1430 spectrophotometer in the 4000–200 cm^{-1} range. The electronic spectra were recorded using a Shimadzu 160 UV–vis spectrometer. The X-band ESR spectra of the complexes

---

* Corresponding author. Tel.: +20 40 3331359; fax: +20 40 3350804.
E-mail address: Yousifchem@yahoo.com (Y.S.Y. El-Sayed).

0022-2860/$ - see front matter © 2009 Elsevier B.V. All rights reserved.
doi:10.1016/j.molstruc.2009.01.042

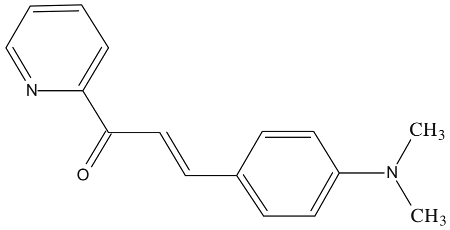

Fig. 1. The structure of chalcone ligand.

were recorded at room temperature on a JOEL-X-band spectrometer equipped with an E 101 microwave bridge. Diphenyl picryl hydrazide free radical (DPPH) was used as internal standard ($g = 2.0023$). The fluorescence measurements were recorded with the aid of Shimadzu RF-510 spectrofluorometer.

Excitation, emission bandwidth, scan rate and excitation wavelength are 10 nm, 100 nm/min and 370 nm, respectively. Magnetic susceptibilities were measured by employing the Faraday balance technique. The equipment was calibrated with $Hg[Co(CNS)_4]$. Diamagnetic corrections were made from Pascal constants. The thermal analysis (TGA) was carried out using computerized Shimadzu TG-50 thermal analyzer up to 800 °C at a heating rate 10 °C/min. in an atmosphere of N_2.

2.3. Computational procedures

All calculations were carried out on a Pentium IV 3.2 GHz machine on windows XP environment using Hyperchem release 7 [23]. The geometry of complex was energetically optimized through molecular mechanics applying MM^+ force field in vacuo with the polka Ribiere (conjugated gradient) algorithm and RMS gradient 0.001 kal/mol followed by molecular dynamics. The optimization is performed without any constrains allowing all atoms, bonds, dihedral angles to change simultaneously. The dynamic simulation was done up to 2000*k* followed by molecular mechanics calculations and same process was repeated five times to ensure the energy minimum had been reached. A bath of relaxation time of 0.1 ps and a step size of 0.001 ps were used for dynamics simulation.

3. Results and discussion

3.1. Study of metal complexes in solution

The reaction of the ligand with metal ions was carried out to establish the most favorable conditions to give increased color intensity and to achieve maximum color development in the quantitative determination of the metal ions. The optimum pH value for the complex formation was detected by scanning the absorption spectra of the complexes using universal buffer solutions. The complexes are formed instaneously and the color of the complexes is stable for 24 h. Temperature exhibits no apparent influence on the color development. The suitable wavelength for the complex formation was also determined and listed in Table 2. The composition of the Cu(II) complexes in solution was established at the optimum conditions described above using the molar ratio (MRM) and continuous variations (CVM) methods. The results indicate the presence of Cu(II) complex in solution having the stoichiometric ratio 1:1 (M:L). The conditional formation constants were calculated using Harvey and Manning equation applying the data obtained from the MRM and CVM methods. The free energy (ΔG^*) of complex formation was also calculated. The limits of validity to Beer's law, molar extinction coefficient, specific absorptivity [24], standard deviation and correlation coefficient were calculated. These values confirmed the possible application of the method for the determination of the metal ions. Ringbom [25] concentration range was also determined and the results are listed in Table 2.

The effect of Cu(II) ions on the emission spectrum of DMAPP was also studied by steady-state emission measurements. The emission spectral patterns of the ligand do not change by adding the metal ion while a decrease in emission intensities was observed as shown in Fig. 2. This implies the absence of emitting excited state complexes. By applying the Stern–Volmer [26] relation:

Table 1
Analytical data of the isolated complex.

No.	Formula	% Elemental analysis				Λ_m[a]	μ_{eff} (BM)	IR spectra (cm^{-1})		Electronic spectra (cm^{-1})		
		C Cal. (F)	H Cal. (F)	N Cal. (F)	M Cal. (F)			$\bar{\nu}_{M\rightarrow N}$	$\bar{\nu}_{M\rightarrow O}$			
1	[CuLXAc]Ac·X	51.06 (51.24)	5.53 (5.64)	5.96 (6.0)	13.5 (13.56)	110	1.72	547	617	28,571	22,222	17,241
2	[CuLXCl]Cl·X	45.39 (45.51)	4.73 (4.8)	6.62 (6.64)	15.01 (14.95)	119	1.78	555	616	26,455	21,978	16,949
3	[CuLXZ]Z·X	34.88 (35.0)	3.63 (3.7)	5.09 (5.1)	11.53 (11.6)	108	1.94	550	629	27,027	21,277	16,667
4	$[CuLX_2]SO_4$	42.86 (42.8)	4.47 (4.43)	6.26 (6.3)	14.19 (14.1)	121	1.80	532	626	28,571	23,256	16,949

L = DMAPP; X = H_2O Z = ClO_4^- Ac = CH_3COO^-.

[a] Ω^{-1} cm^2 mol^{-1}.

Table 2
Analytical parameters for chalcone (DMAPP) complexes.

Parameter	Complex 1	Complex 2	Complex 3	Complex 4
λ_{max} (nm)	570	560	560	563
Buffer	Universal	Universal	Universal	Universal
pH	3.2	3.0	3.5	3.2
Log β_n	4.996	4.998	5.246	4.799
ΔG^*	6.813	7.225	7.323	6.413
Molar absorptivity, ε (dm^3 mol^{-1} cm^{-1})	32,715	33,412	33,752	33,515
Specific absorptivity, a (g^{-1} cm^{-1})	515	618	623	641
Standard deviation	0.0791	0.0781	0.0663	0.0651
Correlation coefficient	0.996	0.996	0.998	0.989
Beer's limits (ppm)	4.0	4.6	5.1	5.0
Ringbom range (ppm)	−0.197–0.253	−0.17–0.244	−0.166–0.333	−0.21–0.343

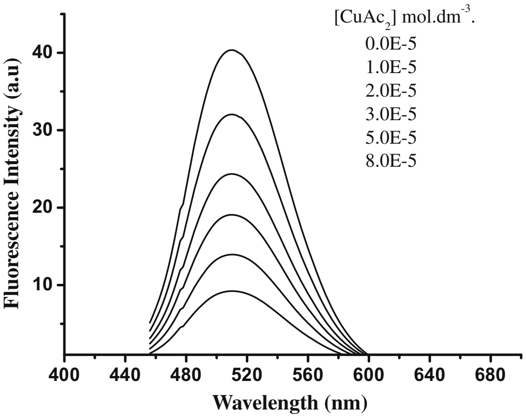

Fig. 2. Fluorescence quenching of 2×10^{-5} mol dm^{-3} DMAPP using Cu^{2+}, acetate in methanol at room temperature.

$$\frac{I_0}{I} = 1 + k_{SV}[Q]$$

where I_o and I represent the fluorescence intensities in the absence and presence of metal ions (quencher), $[Q]$ is the concentration of quencher and k_{SV} is the second-order quenching rate constant; the Stern–Volmer plot as shown in Fig. 3,is not linear, indicating a static type mechanism via ground-state complex formation between DMAPP and Cu(II) ions [27].

Fluorescence quenching of 1×10^{-5} mol dm^{-3} DMAPP by Cu(II) salt with different anions (acetate, chloride, perchlorate and sulphate) have been studied in some alcoholic solvents (e.g. methanol, ethanol, *n*-propanol and *n*-butanol) at room temperature. As shown in Fig. 3, the Stern–Volmer plots are not linear and the quenching efficiency increases in the order of MeOH > EtOH > *n*-PrOH > *n*-BuOH. This is may be attributed to the solvent viscosity and the quenching is diffusion controlled process [28].

The electronic absorption spectra of 1×10^{-5} mol dm^{-3} DMAPP when adding different concentrations of Cu(II) ions of different anions (acetate, chloride, perchlorate and sulphate) have been studied in different alcoholic solvents (e.g. methanol, ethanol, *n*-propanol and *n*-butanol). The absorption spectrum of DMAPP changed when metal ion is added (Fig. 4a) where the initial absorption band of DMAPP decreased on adding the metal ion and a new absorption band appears with a clear isosbestic point at 482 nm in methanol using Cu(II) acetate, chloride, perchlorate and shifted to 484 nm for Cu(II) sulphate, indicating a single equilibrium in solution.

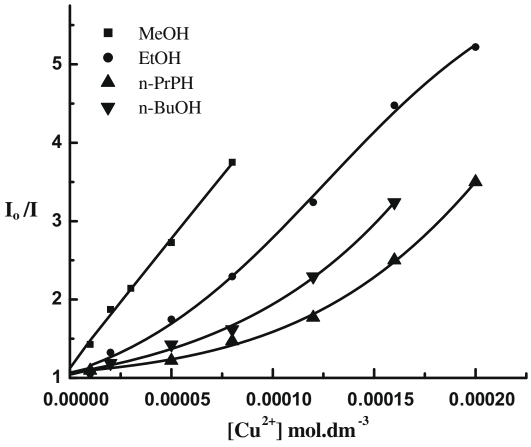

Fig. 3. Stern–Volmer plots for fluorescence quenching of 1×10^{-5} mol dm^{-3} DMAPP in different alcoholic solvents using CuAc$_2$ at room temperature.

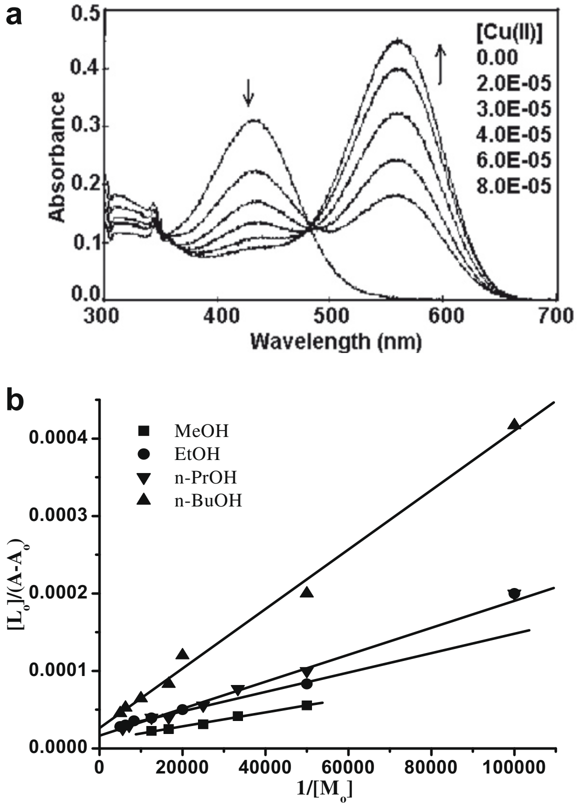

Fig. 4. (a) Absorption spectra of CuAc$_2$ complex with 1×10^{-5} mol dm^{-3} DMAPP in MeOH at room temperature. (b) Plot of $(L_o)/(A - A_o)$ vs. $1/[M_o]$ in different alcoholic solvents at room temperature (20 °C).

The stability constant of the complexes was estimated from the following equation [29,30]:

$$\frac{[L_o]}{A - A_o} = \frac{1}{\varepsilon_{ML} - \varepsilon_L} + \frac{1}{(\varepsilon_{ML} - \varepsilon_L)K[M_o]}$$

where A_o and A are absorbance's of the free DMAPP solution and that with metal complex at a given wavelength; ε_L and ε_{ML} are the molar extinction coefficients of the DMAPP and the metal complex, and $[L_o]$ is the initial concentration of DMAPP. The stability constants (K) values for the complexes of DMAPP with Cu(II) ion in different alcoholic solvents (MeOH, EtOH, *n*-PrOH and *n*-BuOH) are calculated from the plots of $[L_o]/(A - A_o)$ vs. $1/[M_o]$ (Fig. 4b) and the values were collected in Table 3. The data indicated that the stability constant decreases with increasing solvent viscosity and are close to the corresponding diffusion rate constant (k_{diff}) values. The values of k_{diff} were calculated by the following equation [31].

$$k_{diff} = \frac{8RT}{2000\eta}$$

The viscosity dependence of k for diffusion-controlled bimolecular reactions is described by [32]:

$$k = A\eta^{-\alpha}$$

where the parameters A and α are assumed to be constants that are invariant with η. Values of α ranging from zero to unity have been reported [33] for a number of bimolecular chemical reactions. A plot of ln k vs. ln η yielded a straight line from which the value of α was calculated, and found between 0.13 and 0.39 for all complexes.

Also, the absorption spectra of Cu(II)–DMAPP complexes in methanol have been studied in the temperature range 20–50 °C. Using Benesi–Hildebrand method [30], the values of the equilibrium constants K of the complexes were estimated (Table 3). The

Table 3
Stability constant (log*K*) of complexes of Cu(II) of different anions in different alcoholic solvents at different temperature and thermodynamic parameters.

Solvent	*T* (°C)	Stability constant of Cu^{2+} complexes				Thermodynamic parameters											
		Ac^-	Cl^-	ClO_4^-	SO_4^{2-}	$-\Delta H°$ (KJ mol)$^-$				$-\Delta G°$ (KJ mol^{-1})				$\Delta S°$ (J mol^{-1} deg^{-1})			
						Ac^-	Cl^-	ClO_4^-	SO_4^{2-}	Ac^-	Cl^-	ClO_4^-	SO_4^{2-}	Ac^-	Cl^-	ClO_4^-	SO_4^{2-}
MeOH	20	4.06	4.09	4.16	4.03	11.1	7.91	5.26	17.9	22.7	22.9	23.4	22.7	39.8	51.1	61.7	16.3
	30	3.98	4.01	4.13	3.95												
	40	3.92	3.99	4.11	3.84												
	50	3.88	3.95	4.07	3.73												
EtOH	20	3.98	4.06	4.12	3.97	–				–				–			
PrOH	20	3.86	4.01	4.09	3.91	–				–				–			
n-BuOH	20	3.77	3.97	4.07	3.84	–				–				–			

stability constant of the complexes decreased with increasing the temperature. The thermodynamic parameters (the enthalpy change ($\Delta H°$), entropy change ($\Delta S°$) and Gibbs free energy $\Delta G°$) were calculated from Van't Hoff equation plot. The plot of the natural logarithm of the equilibrium constant measured for a certain equilibrium vs. the reciprocal of temperature gives a straight line, the slope of which is the negative of the $\Delta H°$ divided by the gas constant and the intercept of which is equal to the $\Delta S°$ divided by the gas constant, then it is possible to determine $\Delta G°$ and the values are reported in Table 3.

3.2. Characterization of the solid complexes

Structure elucidation of Cu(II) complexes was accomplished on the basis of elemental analyses, IR, UV–vis, ESR spectra, conductance and magnetic measurements as well as the thermal analysis (TGA). The analytical data of the isolated solid complexes are given in Table 1 which is in a good agreement with the proposed structure. The solid complexes were found to be stable in air and soluble in most organic solvents. The high molar conductance values of the isolated complexes measured in DMF solution (10^{-3} M) at room temperature suggested their ionic nature [34] indicating that the anion is present outside the coordination sphere.

A comparison of the IR spectrum of the free chalcone ligand (DMAPP) with those of its metal complexes was carried out to investigate the mode of bonding between the chalcone ligand and Cu(II) ion. In the IR spectrum of the free ligand, the band at 1661 cm^{-1} characteristic for C=O bond was shifted to lower frequency by 6–19 cm^{-1} upon coordination to the metal ions with the appearance of another mode of vibration at 541–547 cm^{-1} corresponding to $\upsilon_{M\leftarrow N}$ bond [35]. The IR spectra of the complexes showed a new band at 617–625 cm^{-1} due to $\upsilon_{M\leftarrow O}$ bond [36] resulting from the interaction between carbonyl oxygen atom and the metal ion. A broad band at 3402–3422 cm^{-1} is present in the spectra of the metal complexes; this band is associated with coordinated and/or hydrated water molecule [37]. The other stretching vibrations of the free chalcone is less affected by complex formation indicating that the chalcone ligand behaves as bidentate ligand via the nitrogen atom of pyridine ring and carbonyl oxygen atom. In the IR spectra of the complexes, bands due to υ_{as} and υ_s of the acetate group are displayed within the ranges 1610–1625 and 1380–1390 cm^{-1}, respectively. This frequency separation is characteristic of monodentate acetate groups for 1:1 (M:L) complexes [38].

The Nujol mull electronic spectra of the Cu(II) complexes under investigation showed bands within the range 26,455–28,571 cm^{-1}. These bands would be assigned to the intra-ligand charge transfer transitions [39] type. The spectra of Cu(II) complexes showed the visible d–d electronic spectral bands within the range 16,667–17,241 cm^{-1}, assigned to $^2B_{1g} \rightarrow {}^2A_{2g}$ transition, characteristic of the square planner geometry of the Cu(II) complex with d_{x2-y2} ground state [40]. This band may be assigned to the transition $^2T_{2g} \rightarrow {}^2E_g$ [39,41].

The Cu^{2+} complexes showed magnetic moments 1.72, 1.78, 1.94 and 1.80 BM for Cu(II) complexes 1, 2, 3 and 4, respectively, indicating the presence of only one unpaired electron [41]. The slightly higher value of observed magnetic moment of Cu(II) complex (3) is consistent [42] with an orbitally non-degenerate ground state of Cu(II) ion.

The ESR spectra of Cu(II) complexes are recorded as poly crystalline samples at room temperature. The *g*-values are taken to calculate the exchange interaction, $G = (g_{||} - 2)/(g_{\perp} - 2)$. According to Hathaway [43], if $G < 4$ a considerable exchange interaction in the solid complexes occurs, while, $G > 4$ indicates that a negligible interaction. The *G*-value of Cu(II) complexes 3 and 4 are 2.15 and 2.0994, respectively. These values leads to spin exchange interaction between Cu(II) ions in the solid state. The $g_{||}$ values in Cu(II) complexes can be used as a measure of the covalent character of metal ligand bond [44]. If the value of $g_{||} < 2.3$, the environment is essentially covalent, but if $g_{||} > 2.3$, the ionic environment is assigned. The $g_{||}$ value of complex 3, showed considerable ionic character while complex 4 is covalent in nature. For complex 1, the hyperfine splitting signals is absent, instead only a single signal appeared. The absence of hyperfine signal may be due to the strong dipolar and exchange interaction between Cu(II) ion in the unit cell [45].

The thermal behavior of the prepared complexes (Fig. 5a) are summarized in Table 4. The Cu(II) complex (1) exhibited the first mass loss in the temperature range 25–120 °C; it may be attributed to the liberation of the hydrated water molecule. The second mass loss at 120–172 °C, is due to the liberation of the coordinated water molecule. The third mass loss at 172–305 °C, is due to the liberation of two acetate molecules. Copper oxide was found as the final product at 305–620 °C. The Cu(II) complexes (2–4) decomposed in three steps. The first step in the range 25–166 °C which may attribute to the loss of hydrated water. The second step in the range 95–420 °C may be due to the liberation of anion in and/or outside the coordination sphere and the CuO formed as a final product in the last step. The kinetic parameters of decomposition process of the complexes namely, activation energy (E^*), enthalpy ($\varDelta H^*$), entropy ($\varDelta S^*$) and free energy of the decomposition ($\varDelta G^*$) as well as the order (n) were evaluated graphically by using Coats–Redfern equations [46].

- Coats–Redfern equation

$$\ln\left[\frac{1-(1-\alpha)^{1-n}}{(1-n)T^2}\right] = \frac{M}{T} + B \text{ for } n \neq 1$$

$$\ln\left[\frac{-\ln(1-\alpha)}{T^2}\right] = \frac{m}{T} + B \text{ for } n = 1$$

where $M = -E/R$ and $B = \ln(ZR/\varphi E)$ where E, R, Z and φ are the activation energy, gas constant, pre-exponential factor and heating rate, respectively.

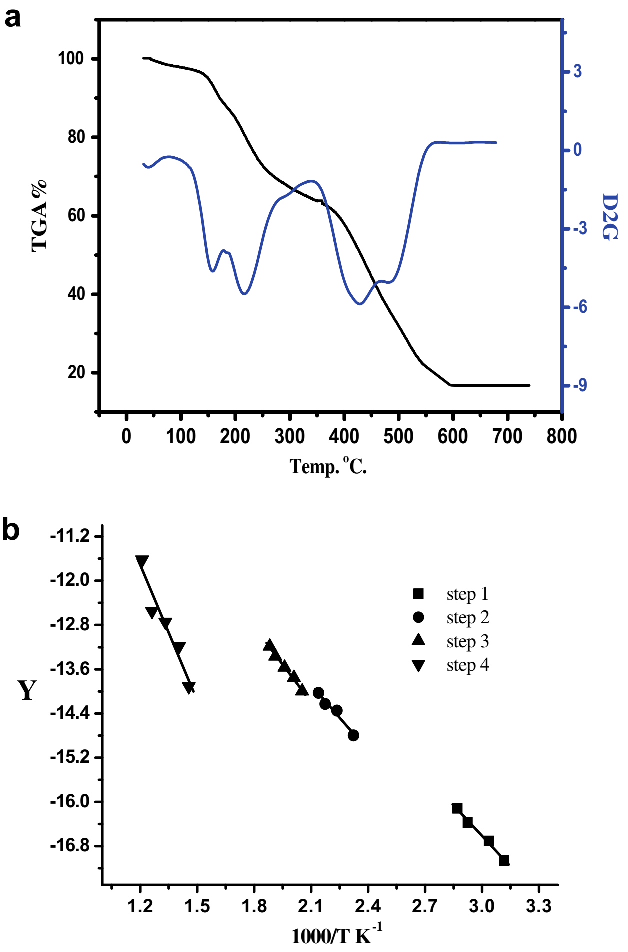

Fig. 5. (a) TGA curve of $CuAc_2$–DMAPP complex. (b) Coats–Redfern plots for the decomposition steps of $CuAc_2$–DMAPP complex: $Y = \ln\left[\frac{1-(1-\alpha)^{1-n}}{(1-n)T^2}\right]$ for $n \neq 1$ or $\ln\left[\frac{-\ln(1-\alpha)}{T^2}\right]$ for $n = 1$.

The correlation coefficient *r* was computed by using the least square method for the above equations. Linear curves were drawn for different values of *n* equal 0, 0.33, 0.5, 0.66 and 1. The value of *n*, which gave the best fit, was chosen as the order parameter for the decomposition stage of interest. The kinetic parameters were calculated from the plots of the L.H.S. vs. 1/*T* of Coats–Redfern equation, as shown in (Fig. 5b). The calculated values of n, E^*, A, ΔS^*, ΔH^* and ΔG^* for the decomposition steps are given in Table 5. From the activation energy values, one can concluded that the water molecules are easy to be eliminated from the complexes according to the following order 4 < 3 < 1 < 2. Also, the energy of activation for the second stage of decomposition for complexes is less than that of the first stage, due to the high steric strain in the intermediate compounds obtained after the first stage of decomposition. The ΔS^* values were found to be negative. This indicates that the activated complex is more ordered than the reactants and/or the reactions are slow [47]. The values of ΔG increase significantly for the subsequently decomposition stages due to increasing the values of $T\Delta S$ from one step to another which override the values of ΔH. This increase reflects that the rate of removal of the subsequent ligand will be lower than that of the precedent ligand [48]. This may be attributed to the structural rigidity of the remaining complex after the expulsion of one and more ligands, as compared with the precedent complex, which requires more energy for its rearrangement before undergoing any compositional change. The positive values of ΔH means that the decomposition processes are endothermic.

Table 4
Thermal decomposition data of Cu(II) DMAPP complexes.

Complex	Temp. (°C)	Mass loss (%)		Assignment
		Estimate	Calc.	
1	25–120	3.5	3.7	Loss of $1H_2O$
	120–172	4.2	4.94	Loss of $1H_2O$
	172–305	24.7	24.9	Loss of 2AcO
	305–620	53.5	51.2	Loss of ligand
2	25–160	8.23	8.5	Loss of $2H_2O$
	160–355	17.1	16.8	Loss of 2Cl
	355–600	55.9	58.2	Loss of ligand
3	25–95	3.53	3.4	Loss of $1H_2O$
	95–380	40.0	39.6	Loss of $1H_2O$, $2ClO_4$
	380–630	46.2	47.1	Loss of ligand
4	80–166	7.82	8.09	Loss of $2H_2O$
	166–420	21.5	21.4	Loss of SO_4
	420–630	54.5	56.3	Loss of ligand

From all of the above observations, the structure of the complexes is given as follows:

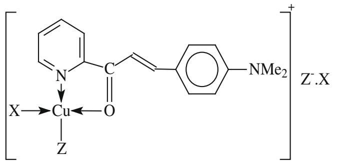

X= H_2O and Z = CH_3COO^- for complex 1
Z = Cl^- for complex 2
Z = ClO_4^- for complex 3.

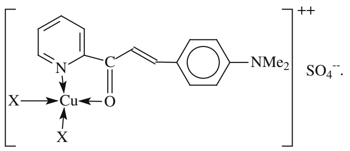

Complex 4.

3.3. Molecular modeling

Since our efforts to obtain crystalline samples of the compounds of X-ray diffraction were unsuccessful, we decided to carry out molecular modeling studies in order to gain a better understanding of all structures. The structures for the Cu-complexes were predicted through strain energy, calculated through the molecular mechanics (MM^+) coupled with molecular dynamics calculations. Although, the molecular mechanics calculations cannot predict the electronic properties, still it has enormous applications in the field of coordination chemistry [49–51]. The molecular mechanics calculate the strain energy, which partition into stretching, bending and torsion and non-bonded interactions for the molecule and give stable structure with least strain energy. It provides an ideal tool to evaluate the degree to which a ligand is structurally organized for metal complexation. Energy minimization was repeated to find the global minimum.

The results of energy minimization of square planar and tetrahedral structures of Cu-complexes without restriction indicate that the strain energies of square planar of Cu(II) complexes are less than that of tetrahedral structures in all cases. This result is in an agreement with the experimental results. Fig. 6 shows the ball and stick model of the optimized geometries of complexes (1–4). The bond lengths (Cu—O)C for complexes 1–4 are 1.728, 1.8, 1.804 and 1.807 Å, respectively, while (Cu—O)H_2 are 1.871, 1.842, 1.844 and 1.841 Å, respectively, in the case of (Cu—N) are 1.875,

Table 5
Temperatures of decomposition and activation parameters (kJ mol^{-1}) of decomposition for the chelates under investigation.

Complex	Steps	T (K)	Coats–Redfern					
			n	r	E^*	ΔH^*	$-\Delta S^{*a}$	ΔG^*
1	1	335.2	1	0.99610	30.6	27.8	0.121	68.2
	2	451.3	1	0.98507	30.9	27.1	0.118	80.3
	3	510	0.66	0.99626	29.9	25.7	0.115	84.2
	4	753.5	1	0.95280	43.6	39.6	0.115	98.2
2	1	375.7	0	0.94543	27.8	24.7	0.105	64.24
	2	442.5	1	0.98436	28.4	24.7	0.113	74.5
	3	510.4	1	0.94917	29.5	25.3	0.114	83.3
	4	747	1	0.96861	25.3	19.1	0.099	93.0
3	1	445.4	1	0.98932	33.5	29.8	0.123	84.7
	2	509.6	1	0.95054	35.7	31.4	0.125	94.9
	3	759.2	1	0.98168	41.9	35.6	0.117	124.7
4	1	330.2	1	0.97110	26.1	23.3	0.117	62.0
	2	486.9	1	0.95695	21.8	17.7	0.096	64.4
	3	618.3	1	0.99753	37.4	32.2	0.114	102.8
	4	930.9	0	0.96025	44.2	36.4	0.105	133.8

[a] KJ mol^{-1} K^{-1}.

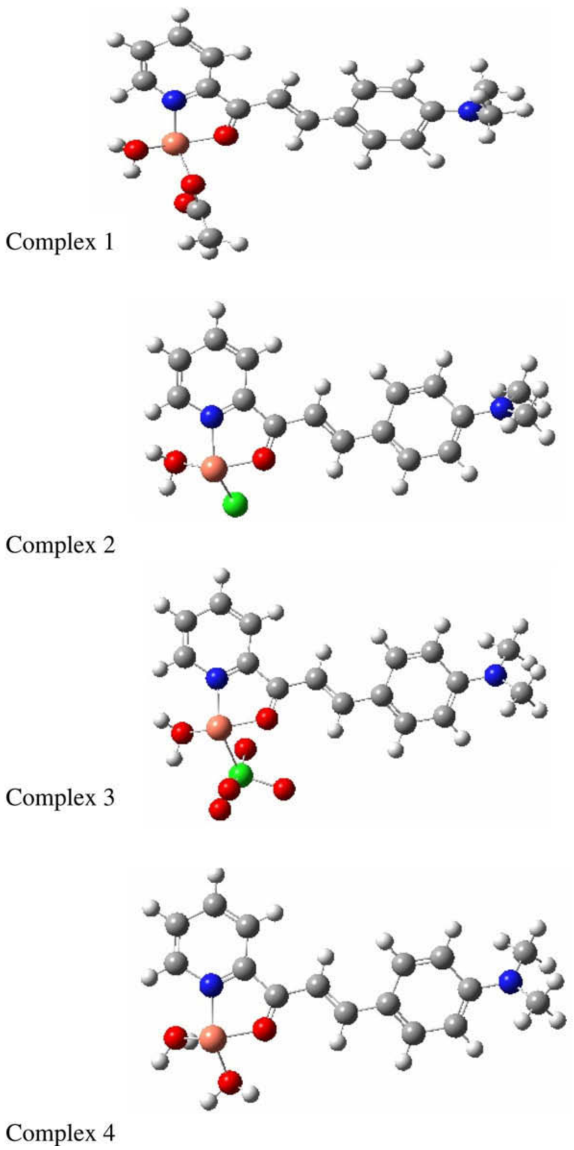
Complex 1

Complex 2

Complex 3

Complex 4

Fig. 6. Ball and stick model of the optimized geometries of complexes (1–4).

1.864, 1.866 and 1.861 Å, respectively, and (Cu—O)Ac for complex 1 is 1.809 Å , (Cu—Cl) for complex 2 is 1.165 Å, (Cu—ClO$_4$) for complex 3 is 1.844 Å. The bond angles of the complexation parts of Cu(II) of different anions with the ligand in the range 75–87° which are stable angles with minimum strain energy.

4. Conclusion

The electronic spectrum of the chalcone (DMAPP) was recorded in methanol. The various optimum conditions for complex formation were detected. The stoichiometric ratios of Cu(II) complexes with DMAPP were determined. The fluorescence of the chalcone was quenched in presence of Cu(II) ions. The calculated Stern–Volmer second order rate constant decreases with increasing the viscosity of the solvent. The solid complexes were prepared and characterized on the basis of elemental analysis, molar conductance, magnetic moments, spectral and thermal studies. The proposed chemical structures of the metal chelates suggested the square planar for all Cu(II) chelate.

Acknowledgement

We are grateful to Dr. M. Khaled for his helpful is the part of theoretical studies.

References

[1] Y.M. Lin, Y. Zhou, M.T. Flavin, W. Nie, F.C. Chen, Bioorg. Med. Chem. 8 (2002) 2795.

[2] D.A.G.C. Pinto, A.M.S. Silva, J.A.S. Cavaleiro, J. Elguero, Eur. J. Org. Chem. (2003) 747.

[3] N. Yayli, O. Ucuncu, E. Aydin, Y. Gok, A. Yasar, C. Baltaci, N. Yildirim, M. Kucuk, J. Photochem. Photobiol. A: Chem. 169 (2004) 228.

[4] D.N. Dhar, The Chemistry of Chalcones and Related Compounds, Wiley, New York, 1981.

[5] G.E. Dubois, G.A. Crosby, R.A. Stephenson, J. Med. Chem. 24 (1981) 408.

[6] M.E. Zwaagstra, H. Timmrman, M. Tamura, Y. Wada, K. Onogi, M.Q. Zhang, J. Med. Chem. 40 (1997) 1075.

[7] K. Krohn, K. Steingrover, M. Srinivasa Rao, Photochemistry 61 (2002) 931.

[8] R. Brouillard, O. Dangles, in: J.B. Harborne (Ed.), The Flavonoids – Advances in Research Since 1986, Chapman & Hall, London, 1994, p. 565.

[9] Y. Goto, Nonlinear Opt. (1992) 225.

[10] S.J. Sun, G. Schwarz, R.H. Kricheldorf, T.C. Chang, J. Polym. Sci. A: Polym. Chem. 37 (1999) 1125.

[11] B. Monroe, W.K. Smothers, E.D. Keys, R.R. Krebs, J.D. Mickish, F.A. Harrington, S.R. Schicker, K.M. Armstrong, D.M.T. Chan, I.C. Weathers, J. Imaging Sci. 35 (1991) 19.

[12] Y. Sato, M. Morimoto, H. Segawa, T. Shimidzu, J. Phys. Chem. 99 (1995) 35.

[13] A.O. Doroshenko, A.V. Grigorovich, E.A. Posokhov, V.G. Oivovarenko, A.P. Demchenko, Mol. Eng. 8 (1999) 199.
[14] K. Rurack, J.L. Bricks, G. Reck, R. Radeglia, U. Resch-Genger, J. Phys. Chem. A 104 (2000) 3087.
[15] N. Marcotte, S. Fery-Forgues, D. Lavabre, S. Marguet, V.G. Pivovarenko, J. Phys. Chem. A 103 (1999) 3163.
[16] P.K. Das, R. Pramanik, D. Banerjee, S. Bagchi, Spectrochim. Acta A 56 (2000) 2763.
[17] Z. Xu, G. Bai, C. Dong, Spectrochim. Acta A 62 (2005) 987.
[18] P. Wang, S. Wu, J. Photochem. Photobiol. A: Chem. 86 (1995) 109.
[19] N. DiCesare, J.R. Lakowicz, Anal. Biochem. 301 (2002) 111.
[20] Y. Wang, J. Phys. Chem. 89 (1985) 3799.
[21] Y.B. Jiang, X.J. Wang, L. Lin, J. Phys. Chem. 98 (1994) 12367.
[22] S.A. El-Daly, M. Gaber, S.S. Al-Shihry, Y.S. El Sayed, J. Photochem. Photobiol. A: Chem. 195 (2008) 89.
[23] HyperChem™, release 7 for Windows, Molecular Modelling system, Copyright© 2002, Hypercube, Inc.
[24] G.H. Ayers, B.D. Narang, Anal. Chim. Acta 24 (1961) 241.
[25] A. Ringbom, Z. Anal. Chem. 115 (1939) 332.
[26] A.M. Braun, M.T. Maurette, E. Oliveros, Photochemical Technology, Wiley, New York, 1991. p. 41.
[27] W.J. Rutter, Acta Chem. Scand. 12 (1958) 438.
[28] S.A. El-Daly, M. Okamoto, S. Hirayama, J. Photochem. Photobiol. A: Chem. 91 (1995) 105.
[29] Y. Sato, M. Morimoto, Hiroshi Segawa, T. Shimidzu, J. Phys. Chem. 99 (1) (1995) 35.
[30] H.A. Benesi, J.H. Hildbrand, J. Am. Chem. Soc. 71 (1949) 2703.
[31] W.R. Ware, J.S. Novrous, J. Phys. Chem. 70 (1966) 3246.
[32] S. Hirayama, H. Yasuda, A.D. Scuily, M. Okamoto, J. Phys. Chem. 98 (1994) 4609.
[33] J.B. Birks, Photophysics of Aromatic Molecules, Wiley/Interscience, London, 1970. p. 497.
[34] W.J. Greary, Coord. Chem. Rev. 7 (1971) 81.
[35] B. Beeccroft, M.J.M. Campell, R. Grazeskowiak, J. Inorg. Nucl. Chem. 65 (1974) 360.
[36] M.A. David, Metal–Ligand and Related Vibrations, Adward Arnold Ltd., London, 1967.
[37] K. Nakamoto, Infrared Spectra of Inorganic and Coordination Compounds, Wiley, New York, 1970.
[38] K. Nakamoto, Infrared and Raman Spectra of Inorganic and Coordination Compounds, Wiley/Interscience, New York, 1986.
[39] L. Dubick, R.L. Martin, Inorg. Chem. 5 (1966) 2203.
[40] P.S. Reddy, K.H. Reddy, Polyhedron 19 (2000) 1687.
[41] M.S. Masoud, O.H. Abdel-Hamid, Z.M. Zaki, Transition Metal Chem. 19 (1994) 21.
[42] B.N. Figgis, J. Lewis, Prog. Inorg. Chem. 6 (1964) 37.
[43] B.J. Hathaway, D.E. Billing, Coord. Chem. Rev. 5 (1970) 143;
B.J. Hathaway, B.J. Dudley, P. Nicholis, J. Chem. Soc. A (1968) 1845;
R.J. Budley, B.J. Hathaway, J. Chem. Soc. A (1970) 1725.
[44] D. Kivelson, R. Nieman, J. Chem. Phys. 35 (1961) 149.
[45] A.K. Mohamed, K.S. Islam, S.S. Hasan, M. Shakir, Transition Metal Chem. 24 (1999) 98.
[46] A.W. Coats, J.P. Redfern, Nature 201 (1964) 68.
[47] C.R. Vinodkumar, M.K. Muraleedharan Nair, P.K. Radhakrishnan, J. Therm. Anal. Cal. 61 (2000) 143;
A.A. Frost, R.G. Pearson, Kinetics and Mechanisms, Wiley, New York, 1961.
[48] P.B. Maravalli, T.R. Goudar, Thermochim. Acta 325 (1999) 35;
K.K.M. Tusuff, R. Sreekala, Thermochim. Acta 159 (1990) 357.
[49] B.P. Hay, R.D. Hancock, Coord. Chem. Rev. 212 (2001) 61.
[50] M. Zimmer, Chem. Rev. 95 (1995) 2629.
[51] S. de Silva, R. de Silva, K. Silva, J. Mol. Struct. (Theochem) 711 (2004) 73.